Available online at www.sciencedirect.com

ScienceDirect

Procedia Structural Integrity 8 (2018) 276–287

Structural Integrity Procedia

www.elsevier.com/locate/procedia

AIAS 2017 International Conference on Stress Analysis, AIAS 2017, 6-9 September 2017, Pisa, Italy

Experimental analysis of tooth-root strains in a sun gear of the final drive for an off-highway axle

A. Terrin[a,b], M. Libardoni[b], G. Meneghetti[b,*]

[a]*Carraro S.p.A., Via Olmo 37, 35010, Campodarsego, PD (Italy)*
[b]*University of Padova, Department of Industrial Engineering, Via Venezia 1, 35121, Padova (Italy)*

Abstract

The force acting on gear teeth can be influenced by several factors such as profile modifications, stiffness variations during meshing, inversion of the sliding direction at the pitch line, tip-to-root interferences, gears and shaft deflections and bearings clearances. Moreover, in planetary gear sets the load can be shared unevenly among the planet gears due to manufacturing inaccuracies of the system. An accurate evaluation of the real load-time history experienced by the teeth is not straightforward and is affected by strong approximations even when advanced simulation software packages are used to create the theoretical model. Therefore, experimental analysis of the behavior of gears under in-service load still constitutes a major step in the development of new transmission systems. In this work, three strain gauges were applied at different positions along the tooth root width of the sun gear mounted in the final drive of an off-highway axle. Strain measurements where then performed during a bench test of the complete axle and the signal was acquired by means of a telemetry system. Finally, the acquired data were used to assess the accuracy of software calculations and to identify the causes of overloads.

Peer-review under responsibility of the Scientific Committee of AIAS 2017 International Conference on Stress Analysis

Keywords: Strain gauges, Gear, Planetary gear set

1. Introduction

The actual pressure distribution along the face of a tooth as well as among different teeth simultaneously in contact during normal operation of spur gears is strongly affected by the manufacturing and assembling accuracy of the shafts, the supports and the gear itself. Moreover, several aspects of the design as well as the operating condition of the system may influence the dynamic behavior of the gear pair. Among these, profile modifications, load, friction properties, speed, and inertia and stiffness of the rotating elements are the most important. Several numerical methods exist to calculate the compliances in gears and shafts and to estimate the amount of misalignment of mating teeth and the meshing stiffness during gears operation. Based on the results of such analysis, the designer may choose an appropriate set of geometry modifications to improve the pressure distribution for the design load and reduce the transmission error. For instance, crowning and helix modification are used to compensate for the effect of bearing clearances and shaft deformations, while tip and root relieves are useful to avoid interferences and abrupt variations of the load due to the passage from single to multiple tooth pair contact during the meshing period. Although calculation software packages are a very useful tool for the determination of an appropriate set of geometry

* Corresponding author. Tel.: +39-049-8276751; Fax: +39-049-8276785.
E-mail address: giovanni.meneghetti@unipd.it

Peer-review under responsibility of the Scientific Committee of AIAS 2017 International Conference on Stress Analysis
10.1016/j.prostr.2017.12.029

modification to ensure the proper functioning of the gear set, numerical results are based upon simplified models which cannot accurately account for all the possible causes of gears overloading. Moreover, the load distribution can be strongly influenced by deviations from the nominal geometry, even when errors are within the prescribed tolerances. Therefore, despite the increasing reliability of computational tools for gear calculation, experimental validation of the numerical models is still fundamental especially in the design of new products. The first experimental works on the dynamics of gear meshing date back to the 50s, when the advent of foil strain gauges and the rapid improvement of signal conditioning systems allowed the first on-line measurements of tooth root strains. Tests were typically conducted in gear boxes appositely developed, and bridge supply and strain signal were transmitted through slip rings (Yeh, 1959; Utagawa and Harada, 1961; Pethick, 1967). The need for experimental data for the validation of calculation models was particularly felt in the aeronautic industry, where weight saving is of primary importance and the consequence of a failure would be catastrophic. Great attention has been drawn by researchers and engineers to planetary gear units, where the simultaneous meshing of the sun gear with three or more planet gears, introduces a high grade of uncertainty in the calculation, since any deviation by the nominal geometry of the system may lead to an uneven distribution of the load among the planet gears, the load sharing being usually worst for higher number of planets. This aspect was investigated experimentally by Hidaka and Terauchi (1976), Oswald (1987), and Krantz (1992), using strain gauges applied at the tooth root of the sun gear and, more recently, by Ligata et al. (2008) by gluing strain gauges in the fixed internal gear. The latter approach is simpler because eliminates the need for current supply to the gauges and for transmitting the signal from a rotating shaft, but on the other hand does not allow to investigate the behavior under load of the sun gear, which often represent the weakest component in the gear set especially regarding pitting failures. The distribution of the load over the width of a single tooth of the sun gear can be analyzed by means of several strain gauges placed along the tooth root (Hidaka and Terauchi, 1976). The same procedure was used also by Handschuh (1997) and Hotait et al. (2011) for hypoid bevel gears and by Baud and Velex (2002) for helical gears.

A crucial aspect in the dynamic measurements of tooth root strain is represented by noise, which may be introduced in the transmission of the un-conditioned signal through the slip rings. In the last years, the availability of multi-channel telemetry systems significantly contribute to improve the quality of measurements on rotating components such as gears (Zhou et al. 2016), by allowing the conditioning of the signal before its wireless transmission.

In this work strain measurements were performed at the tooth root of a sun gear in a planetary gear set of a steering axle used in agricultural vehicles (Figure 1.a). One of the main cause of failures of axles for off-highway vehicles is pitting on the sun gears of planetary gear sets, which the final drive of the transmission consists of (Figure 1.b). The onset of pitting is detrimental causing noise and vibrations.

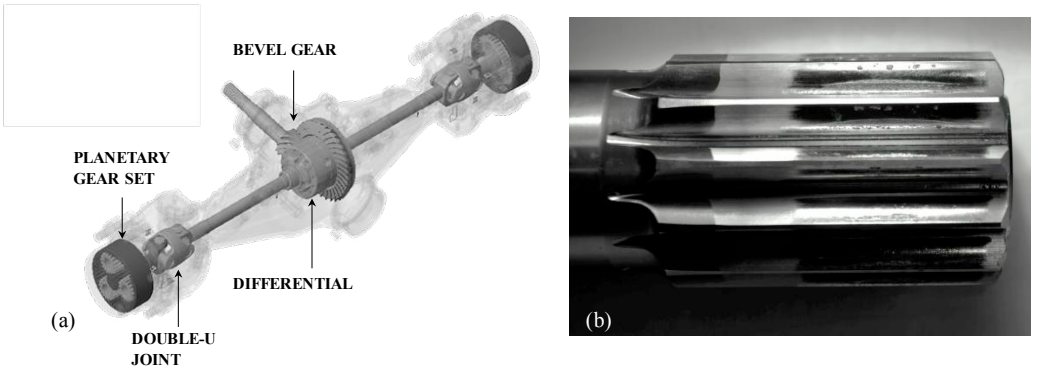

Figure 1. a) Scheme of an off-highway axle. b) sun gear damaged by pitting.

The sun gear is connected to the drive shaft through a double-U joint and meshes with three planets gears mounted on needle bearings and supported by pins fitted by interference to the wheel hub, which forms the planet carrier. The construction quality of the planet carrier, in terms of design and manufacturing accuracy, is perhaps the most important factor to guarantee the structural integrity of the drive. The deflections under load of the carrier and the pins, as well as positioning errors of the pins due to manufacturing or assembling defects may strongly influence the load sharing between the planet gears and the pressure distribution on gears teeth and bearings, considerably reducing the life of the components. Particularly, the assembly of the pins by press fit inevitably implies a certain degree of perpendicularity error. In this work, three strain gauges were placed at the root of the driving flank of a sun gear tooth to analyze the load-time history on the tooth and indirectly evaluate the pressure distribution along the gear width. Signal conditioning and transmission were provided by a multi-channel telemetry system. Data were then compared with the results of a simulation model of the final drive.

2. Test set-up

The Four-Square Test (FST) bench is a power recirculating rig designed to investigate the structural durability of gears and bearings of axles (Figure 2). Two axles are positioned with their input shafts facing each other, and mechanically connected by means of a cardan shaft driven by an electric motor. On each side of the bench, a pair of sprockets connected by a chain is mounted on the wheel hubs of the axles. The cardan shaft is preloaded to impose a given applied torque to one of the two axles (hereby addressed as the main axle), while the second (auxiliary) axle closes the kinematic chain recovering the power. Thus, operation under high wheel torques can be simulated with limited energy consumption. Torque, speed and lubricant temperature are measured during the test, lubricant cooling being provided by fans when the temperature set point is exceeded.

In the present work, three strain gauges were applied along the tooth root of the left-side sun gear of the tested axle during the test (Figure 3). The sensors had a grid length of 0.2 mm and were glued within the 30 mm portion of the tooth width interested by the contact with the planet gear; the center of the grid was shifted from the tooth root in the direction of the driving flank, as reported in Figure 4.

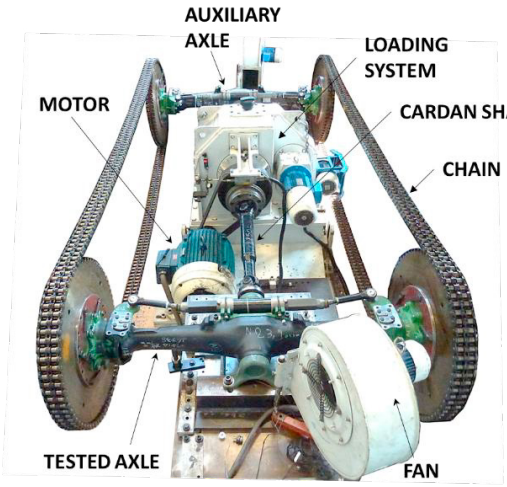

Figure 2. Four Square Test set-up.

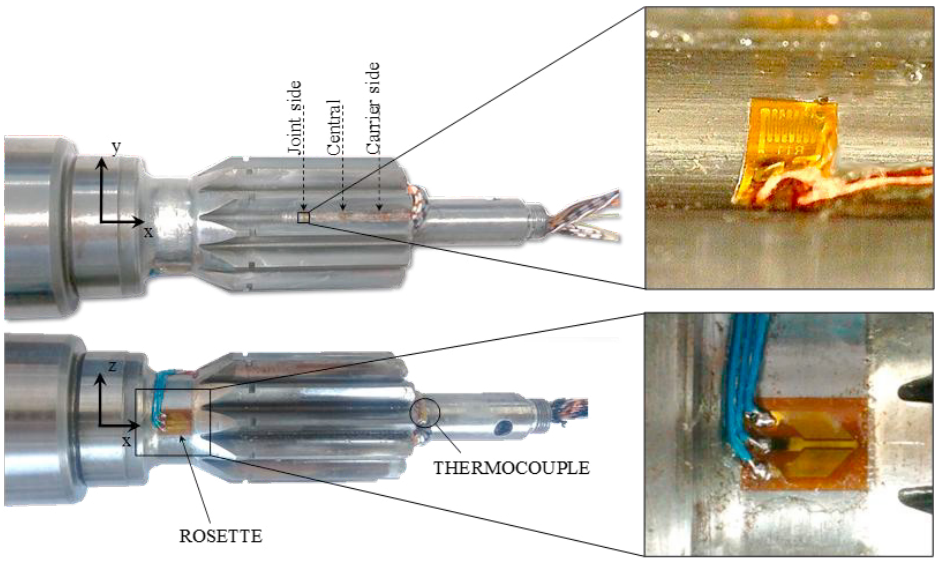

Figure 3. Strain gauges applied to the sun gear.

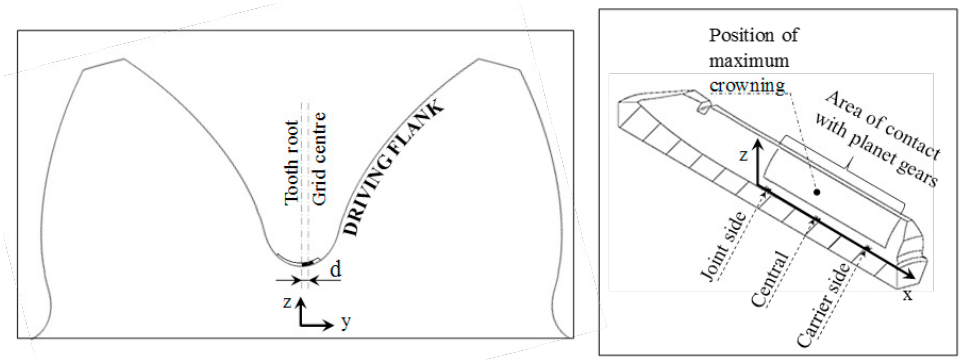

Figure 4 . Position of the strain gauges along the tooth root.

The actual position of the strain gauges after the application, with reference to Figure 4, was verified with an optical microscope and is reported in Table 1. Because of the high strain gradient along the fillet radius of the tooth root, the possible error in the strain measurement due to the ±0.1mm uncertainty in the strain gauge position was estimated by a finite element analysis of the sun gear and resulted to be as high as ±15%.

Table 1. Position of strain gauges along the tooth root (see Figure 4).

	Position along the x axis [mm]	Distance from the tooth root, d [mm]
Joint side	1.0 ± 0.2	0.1 ± 0.1
Central	13.0 ± 0.2	0.1 ± 0.1
Carrier side	26.0 ± 0.2	0.2 ± 0.1

Two combined ±45° rosette were applied between the gear and the double-U joint, to measure the input torque in the final drive. Finally, a T-type thermocouple was used to monitor the oil temperature inside the drive and to avoid overtemperature above 80°C.

Bridge signals and supply were transmitted by means of a KMT-MT32 multi-channel telemetry system to a IMC-CRONOS-PL2 acquisition unit. The system is composed by a battery and seven modules for signal conditioning (three modules for the tooth gauges, one for the torsion bridge and one for the thermocouple), the collection of data from the various channel (one module) and the transmission of the signal to the acquisition unit (one module). Strain gauges were connected to the cables coming from the telemetry modules by means of thin wires (0.14 mm diameter) fixed along the tooth root. Then a hollow shaft was mounted with interference fit in the sun gear to allow the passage of the cables out of the carrier (Figure 5).

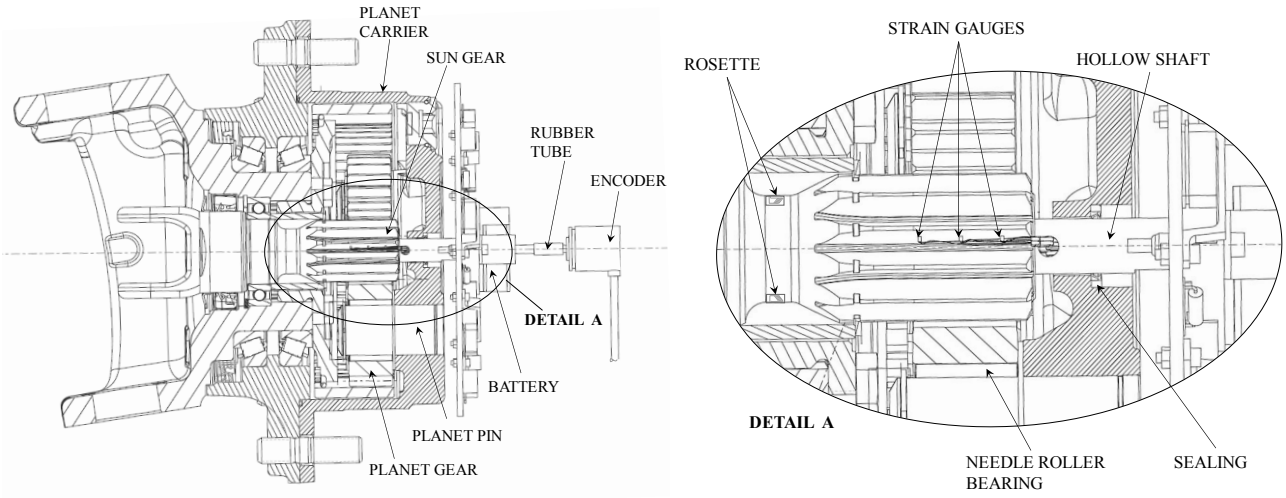

Figure 5. Scheme of the final drive and the measurement set-up.

The telemetry modules were disposed circumferentially on an aluminum plate coaxially screwed to the shaft (Figure 6). The battery was fixed in correspondence of the center of the plate. A rubber tube connected a pin placed upon the battery support to the shaft of an incremental encoder. The stator was held by a support bracket fixed to the rig frame, therefore the encoder measured the absolute angle of rotation of the sun gear since the start of the test. In order to know the exact position of the sun gear with respect to each planet at any time during the test, the angular position of the gauged tooth was marked in the aluminum disc and its relative position with respect to the carrier was adjusted before each acquisition session.

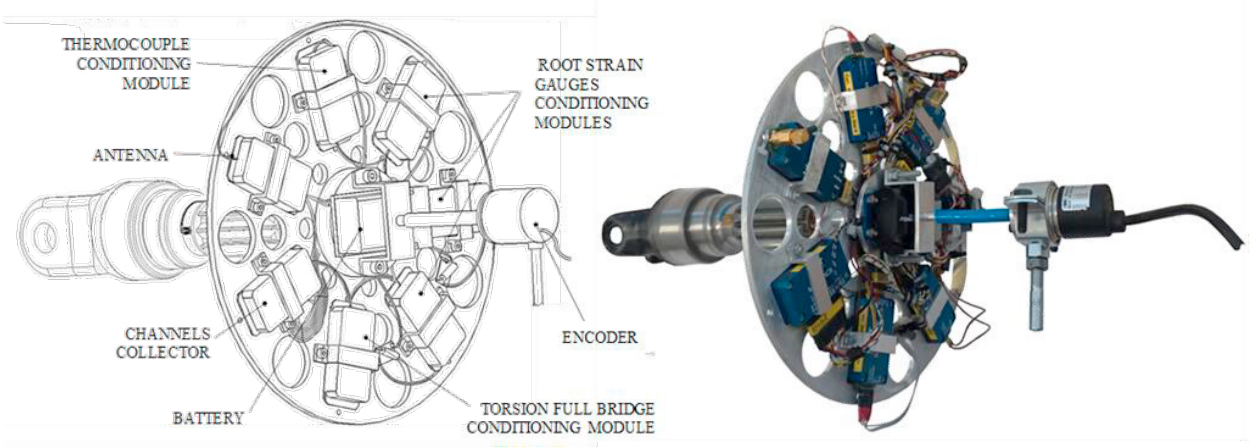

Figure 6. Assembly of the aluminium plate carrying the telemetry modules.

3. Calculation model

Fatigue assessments against pitting failures according to ISO standard 6336 (2006), is based on the condition:

$$\sigma_H < \sigma_{HP} \tag{1}$$

where σ_H is the maximum contact pressure occurring on the tooth face during meshing, whilst σ_{HP} is a permissible value of pressure which depends on the material, the target life and the operating condition of the gears in terms of surface finish, speed and type of lubricant.

The value of the maximum contact pressure is evaluated through the equation:

$$\sigma_H = \sigma_{H,nom} \sqrt{(K_A \cdot K_V \cdot K_{H\beta} \cdot K_{H\alpha} \cdot K_\gamma)} \tag{2}$$

In equation (2), $\sigma_{H,nom}$ represents the nominal contact pressure in the position along the portion of the tooth profile within which the load is carried by a single pair of teeth, where the difference between the curvature radii of the two mating surfaces is maximum. Then, K factors are introduced to account for all the potential causes of overloads. More in detail:

- $K_{H\beta}$ accounts for gaps between the contact surfaces along the tooth width caused by crowning, gears and shaft compliances, and misalignments due to bearing clearance and manufacturing errors, which may reduce the contact area causing substantial modifications to the Hertzian pressure distribution.
- $K_{H\alpha}$ accounts for the effect of the uneven distribution of load between simultaneously contacting tooth pairs, due for example to pitch errors or inaccuracies in the profile geometry.
- K_A accounts for possible overloads caused by the driven or the driving machines
- K_V accounts for internal dynamic perturbances.
- K_γ accounts for the possible uneven distribution of the load among the three planet gears of the final drive.

K factors are under the square root in equation (2) because teeth are assimilated to a pair of cylinders and therefore it is assumed that the contact pressure depends on the square root of the force as predicted by the theory of Hertz (Johnson, 1987).

Among the listed factors, $K_{H\beta}$ is considered as the most influencing with respect to pitting failures. The Annex E of ISO6336 provides an iterative calculation method which allows to evaluate with reasonable accuracy the distribution of normal force along the pitch line. Several software packages for gear Tooth Contact Analysis (TCA) have been developed over the years to allow a more comprehensive evaluation of the effect of misalignments and gear microgeometry on the whole tooth face. In this work, a model of the planetary gear set was created by the software KISSsoft, to compute the line load distribution on the sun gear teeth. Figure 7 shows the line load distribution along the tooth face, calculated in correspondence of the Highest Point of Single Tooth pair Contact of the sun gear for a input torque to the final drive $T_s = 520\ Nm$. Such location was chosen for convenience in the comparison with the experimental data, as clarified in section 4. The calculation accounts for the compliances of gears and shafts, the geometry modifications such as crowning, and the bearing clearances. Since sun and planet gears are crowned, the contact pressure between the teeth surfaces is maximum in correspondence of the center of the elliptical contact area, whose position depend on the relative alignment between the gear axes, and decreases in both directions along the tooth width. Being tooth height much smaller with respect to its width, the load distribution affects the strain along the tooth root, therefore the measures of the three strain gauges can be used to assess, at least approximately the position of maximum pressure and hence verify the relative alignment of each planet gear and the reliability of the calculation model.

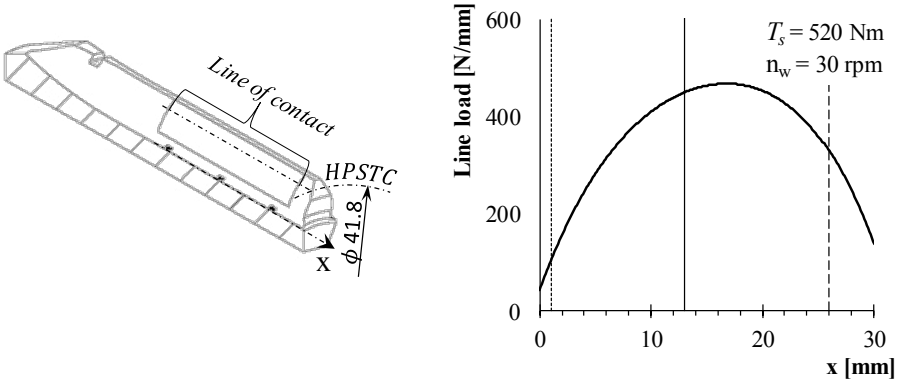

Figure 7.Line load distribution calculated by the KISSsoft model.

4. Experimental data

Among the factors listed in section 3, the most influencing for the pitting durability of planetary gear sets in agricultural axles are the uneven distribution of load over the face width (quantified by the ISO standard with the factor $K_{H\beta}$) and among the three planet gears (quantified by the factor K_γ). As mentioned in the previous section, the non-uniform load distribution along the tooth produces differences among the strains measured by the three gauges, while the load sharing among the planet gears would result in a different strain pattern when the tooth meshes with the three planets. Concerning the other possible causes of non-uniform strain patterns, for accurately manufactured gears with appropriate profile modifications and high specific loading, usually $K_{H\alpha}$ is less significant and therefore will not be analyzed in the following. Also factors K_A and K_V are typically negligible for this kind of application, since during the four-square test the axle is driven by a constant torque at relatively low speeds.

Figure 8 shows the typical strain pattern measured by the gauge placed in the central position, versus the angle of relative rotation of the sun gear with respect to the carrier. The measure was performed with an input torque to the final drive of $T_s = 520\ Nm$ and a wheel speed $n_W = 30\ rpm$. For easiness of comprehension the zero of the x-axis in the chart was placed in correspondence of the start of meshing of the gauged tooth with a planet gear (see Figure 9). Then, since the encoder measures the absolute angle of rotation of the sun gear γ, while the carrier rotates at 1/τ the sun speed in its same direction, the relative angle γ_r is computed as:

$$\gamma_R = \gamma \cdot \frac{\tau + 1}{\tau} \tag{3}$$

Where τ is the transmission ratio of the final drive. Thus, in the relative reference system, the period between two consecutive meshing of the considered sun tooth is equal to the angular spacing of the three planets, namely 120°

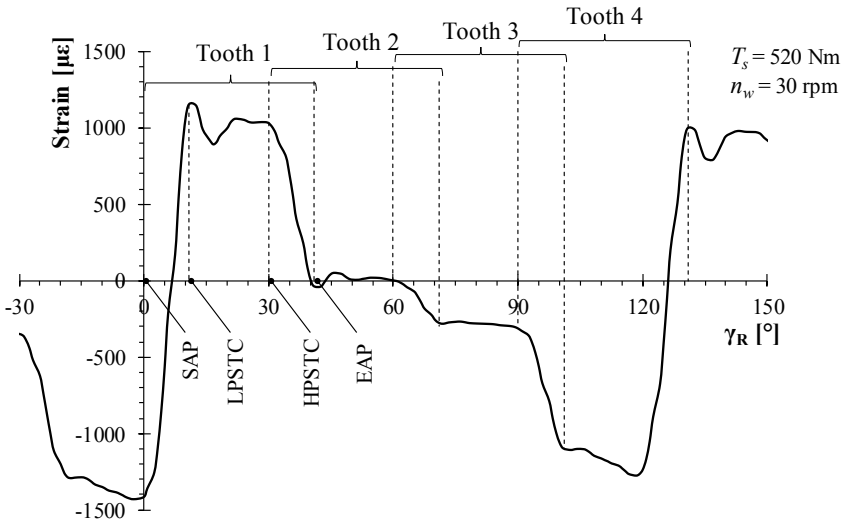

Figure 8. Strain pattern (central gauge).

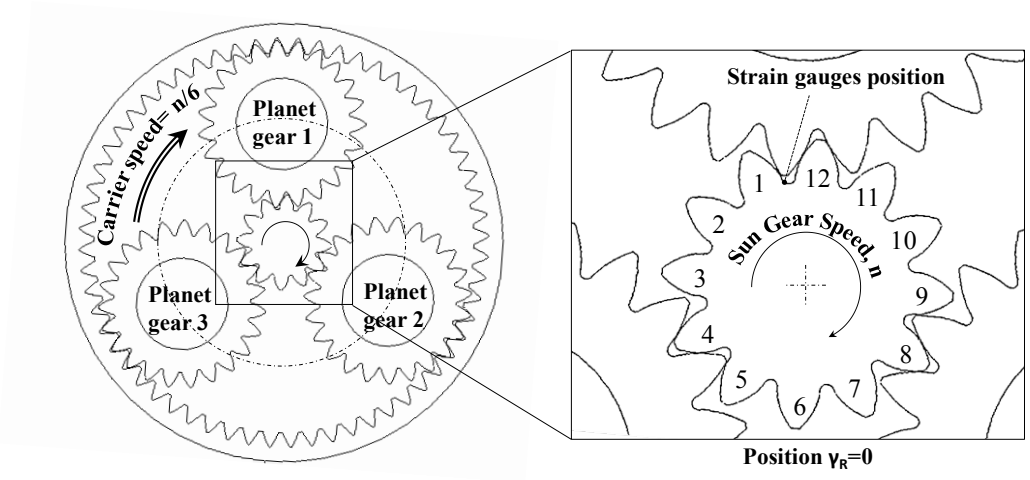

Figure 9. Scheme of the planetary gear set.

With reference to the configuration defined in Figure 9 and Figure 10, the strain-time history can be interpreted as follows:

- The gear covers an angle of about 41° during the period of meshing of a tooth pair, between the Start of Active Profile (SAP) and the End of Active Profile (EAP)
- Considering the gauged tooth (tooth 1), the strain rapidly increases during the first 11° of rotation, until the Lowest Point of Single Tooth pair Contact (LPSTC), while tooth 12 is gradually unloaded.
- Between the lowest and the Highest Point of Single Tooth pair Contact (HPSTC) the curve is altered because the direction of mutual sliding between the mating teeth and therefore the direction of friction forces reverses in correspondence of the pitch point.
- In correspondence of the HPSTC the strain drops because tooth 2 engages and therefore tooth 1 is gradually unloaded within the following 11°.
- In the coordinate system relative to the carrier, the sun gear covers 120° before tooth 1 encounter a new planet gear. The strain reaches very high compressive values when tooth 12 is loaded.

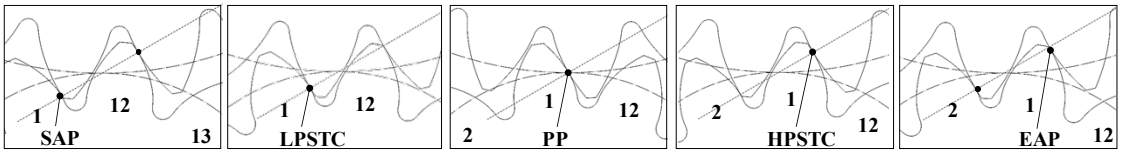

Figure 10. Sequence of meshing between sun and planet gear.

The signal of the three gauges are shown in Figure 11 for a complete revolution of the planet relatively to the carrier. Considering the strain gauges in the joint and carrier sides, the strain pattern measured during the meshing with planet gear 1 is considerably different with respect to the one observed during the meshing with planet gears 2 and 3.

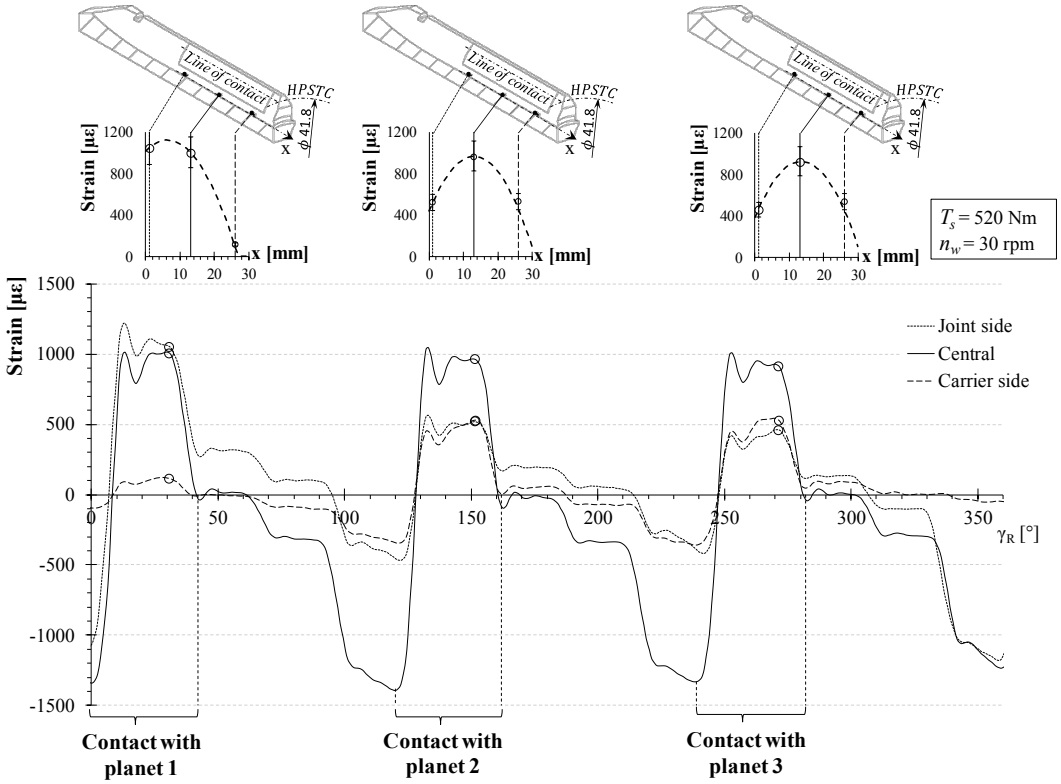

Figure 11. Strain patterns at three different position along the face width. The upper charts report the values of strain relevant to the contact with the three planet gears, when the contact occurs at the HPSTC of the sun gear.

The strain measured by the three gauges in correspondence of the contacts with the three planets at the HPSTC of the sun gear are reported in Table 2. Strain values relevant to contacts with the three planet gears, in correspondence of the HPSTC of the gauged tooth. Such location is considered as reference because it is easily recognizable in the chart and is relatively far from the pitch line, where the change in the direction of friction forces causes a perturbation in the strain pattern. It can be noted that the values measured by the strain gauge in the central position are quite repeatable, with a difference among the values measured in correspondence of the contact with the three planet gears lower than 8%. However, the two lateral gauges measure very different strain values during the contact with the first planet as opposed to those registered in the contact with the second and third planet gears. It could be verified that this behavior is repeatable in the subsequent revolutions.

Table 2. Strain values relevant to contacts with the three planet gears, in correspondence of the HPSTC of the gauged tooth.

		Contact with planet gear 1	Contact with planet gear 2	Contact with planet gear 3
STRAIN [με]	Joint side	1048	518	461
	Central	1004	967	927
	Carrier side	113	528	537

In the upper part of Figure 11, the strain values reported in Table 2, are shown in correspondence of the contact with each planet gear. The parabolic interpolation of the strain values highlights the different load distribution in the three cases: it is reasonable to suppose that the strain observed in the contact with planet gears 2 and 3 could be originated by a line load distribution with a maximum value near to the position of the central gauge as predicted by the calculation model. On the contrary in the contact with planet gear 1 the maximum load is probably shifted between the position of the central and the joint side strain gauges. The evaluation of the actual load distribution from the measured root strain is further developed in the following.

5. Discussion

The relatively good repeatability of the strain pattern measured by the central gauge suggests that the differences in strain during the contact with the three planet gears would be caused more by differences among the alignments of the pins, rather than to an uneven sharing of the load among the three planets. This is in agreement with Oswald et al. (1987) and Krantz (1992) who observed that for gear sets with three planets and number of teeth of the sun gear multiple of three, the load is typically shared quite evenly among the planet gears. Therefore, an attempt was made to estimate the line load distribution along the tooth face compatible with the signal of the strain gauges. The procedure followed to assess the face load distribution is the following:

- a parabolic distribution for both the strain along the tooth root and the line load on the tooth face was assumed:

$$\varepsilon_{root} = ax^2 + bx + c \tag{4}$$

$$L = ux^2 + vx + z \tag{5}$$

- the equations of the root strain parabolas relevant to the contact with each planet were determined from the three strain values measured in correspondence of a contact at the HPSTC. From the equation of each strain parabola the position of the maximum strain along the tooth root was determined as:

$$x_{max} = -\frac{b}{2a} \tag{6}$$

  Note that this position corresponds to the point of maximum strain provided that the strain values used for the determination of the equation are all measured along the same line parallel to the sun gear axis. Therefore, in this phase, the values measured by the strain gauge in the carrier side were scaled by a factor 0.85 to account for the different position of the center of its grid with respect to the others, as reported in Table 1. The scale factor was estimated from the results of a FE analysis.
- the maximum line load was assumed to occur approximately at the same coordinate x_{max}, as the maximum strain, therefore:

$$-\frac{v}{2u} = x_{max} \tag{7}$$

  Or

$$v = -2ux_{max} \tag{8}$$

- Assuming that the load is evenly distributed among the planet gears ($K_\gamma \approx 1$), the integral over x of the line load, within the face width b of the planet gear must equal the normal load F_n:

$$F_n = \int_{x_{L1}}^{x_{L2}} (ux^2 + vx + z)dx \tag{9}$$

  Where x_{L1} and x_{L2} are defined as follows:

$$x_{L1} = \max\left[0, \quad \frac{-v + (v^2 - 4uz)^{0.5}}{2u}\right] \tag{10}$$

$$x_{L2} = \min\left[30, \quad \frac{-v - (v^2 - 4uz)^{0.5}}{2u}\right] \tag{11}$$

  In other words, since the load cannot assume negative values, the integral is evaluated only between the roots of the parabola if they are included within the interval $0 \le x \le 30\ mm$. Therefore:

$$\frac{1}{3}u({x_{L2}}^3 - x_{L1}^3) + \frac{1}{2}v({x_{L2}}^2 - x_{L1}^2) + z(x_{L2} - x_{L1}) = F_n \tag{12}$$

  Or, combining eq (8) and (12):

$$z = \frac{\left[F_n - \frac{1}{3}u({x_{L2}}^3 - x_{L1}^3) + u x_{max}({x_{L2}}^2 - x_{L1}^2)\right]}{(x_{L2} - x_{L1})} \tag{13}$$

The normal force generated at the HPSTC of the sun gear tooth can be calculated according to appendix A. Note that the sun gear torque should be divided by three to account for the load sharing among the three planet gears.

- The values of the coefficient v and z are given by equations (8) and (13). Moreover, the experimental data clearly shown that the entity of the crowning is such that the line load parabola has a downward concavity (u is negative). Thus, various parabolic load distribution may be derived changing the value of the first coefficient u. Note that, for a chosen value of u, z may depend on x_{L1} and x_{L2}, which in turn depend on z. However, the problem may be solved iteratively using $x_{L1} = 0$ and $x_{L2} = 30$ as seeding values to compute z, then x_{L1} and x_{L2} may be calculated and used to derive a new value of z. Usually the calculation converges in few iterations.

- Finally, a finite element model of the sun gear was built to find the value of u relevant to the load distribution that, applied to the model in correspondence of the diameter of HPSTC along with the relevant friction force (see appendix A), produces the least square error between the measured root strain and the results of the analysis. A friction coefficient of 0.05 was assumed, which is a typical value adopted for gear calculations (Bower, 1988).

Figure 12 shows the line load distribution computed with the above procedure and the comparison among the tooth root strain resulted by the finite element model and the experimental data, represented along with the relevant error bands as defined in section 2.

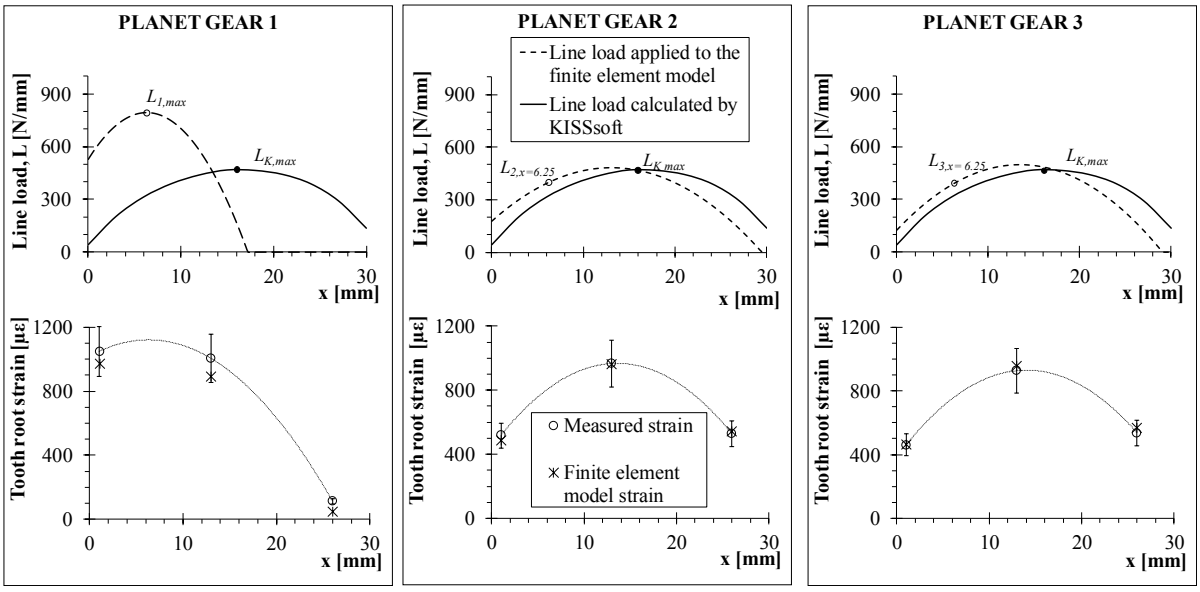

Figure 12. Comparison between the line load distribution calculated by the software KISSsoft, and the parabolic line load distribution which produces the least square error among the measured values of strain and the results of the finite element model.

Note that the very good agreement between output of the finite element calculation and measured strain values supports the hypothesis that the load sharing factor K_γ is almost unitary. The calculated line load distributions for planet gear 2 and 3 are similar and reach a maximum value close to the one calculated by the KISSsoft model, $L_{K,max}$. On the contrary, the contact with the first planet results in a maximum value of line load $L_{1,max}$ 69% higher than $L_{K,max}$. It is worth noting that the fatigue curve suggested by the ISO standard 6336 for the evaluation of the pitting durability of case hardened gears are based on a relation of the type:

$$\sigma_H{}^{13.22} N = c \tag{14}$$

Where c is a constant that depends on the material quality and N represent the expected pitting life (in terms of number of contact cycles) of a gear subjected to the maximum contact pressure σ_H which is proportional to $L^{0.5}$. The damage calculated by KISSsoft for a given number n of contact cycles sustained by a sun gear tooth can be expressed in the form n/N_K , where N_K represents the life relevant to the contact load $L_{K,max}$. However based on the experimental results, seems more appropriate to compute the damage in correspondence of the coordinate $x = 6.25\ mm$ where the pressure generated by the contact with the first planet gear is maximum. At this location, the sun gear tooth is subjected to a line load 69% higher than $L_{K,max}$ during the contact with the first planet gear and 15% and 18% lower than $L_{K,max}$ in the contact with planet gear 2 and 3, respectively. Thus, considering a linear damage sum according to the Palmgren-Miner rule, as suggested by the ISO standard for life calculations under variable amplitude loading conditions, the damages accumulated by the tooth in n contact cycles is given by

$$\frac{\frac{1}{3}n}{N_K\left(\frac{L_{1,max}}{L_{Kmax}}\right)^{-\frac{13.22}{2}}} + \frac{\frac{1}{3}n}{N_K\left(\frac{L_{2,x=6.25}}{L_{K\,max}}\right)^{-\frac{13.22}{2}}} + \frac{\frac{1}{3}n}{N_K\left(\frac{L_{3,x=6.25}}{L_{K\,max}}\right)^{-\frac{13.22}{2}}} = \frac{n}{3N_K}(1.69^{6.61} + 0.85^{6.61} + 0.82^{6.61}) = 10.9\frac{n}{N_k} \tag{15}$$

Therefore, the service life of the sun gear, is expected to be more than 10 times lower than that predicted assuming the line load distribution resulted by the theoretical model for all the three planets.

6. Conclusions

Three strain gauges were applied at different position along the tooth root of the sun gear in a planetary gear set for off-highway axle. Strain measurement were performed during a bench test of the complete axle by means of a telemetry system. Then, a procedure was developed to evaluate the line load distribution along the width of the tooth based on the signal measured by the three strain gauges, in order to assess the accuracy of a calculation model developed through the commercial software KISSsoft. The results show that while the maximum line load generated in the contact with two of the three planet gears is in good agreement with the output of the calculation model, the contact with the first gear produces a maximum value of the line load distribution evaluated at the HPSTC 69% higher. Such over-load effect is to be attributed to a misalignment of the planet gear due to the manufacturing process of press fit of the pin in the planet carrier and could considerably reduce the pitting durability of the final drive.

Acknowledgements

The authors would like to acknowledge Carraro S.p.A. for making the four-square test bench available for the present work.

Appendix A. Calculation of normal and friction force

In driver gears friction forces are always directed toward the tooth root in the dedendum, vanish in correspondence of the pitch line and assume the opposite direction within the addendum. Figure 13 shows the force applied at the HPSTC of a driver spur gear tooth, decomposed into its normal and friction components. For a given driving torque T_1, the equilibrium condition with respect to the pole O_1 is given by

$$T_1 = F_n\left(r_{b,1} + \rho_{HPSTC,1} \cdot \mu\right) \tag{16}$$

Therefore, the normal force can be calculated as:

$$F_n = \frac{T_1}{\left(r_{b,1} + \rho_{HPSTC,1} \cdot \mu\right)} \tag{17}$$

And the friction force is given by

$$F_f = F_n \cdot \mu \tag{18}$$

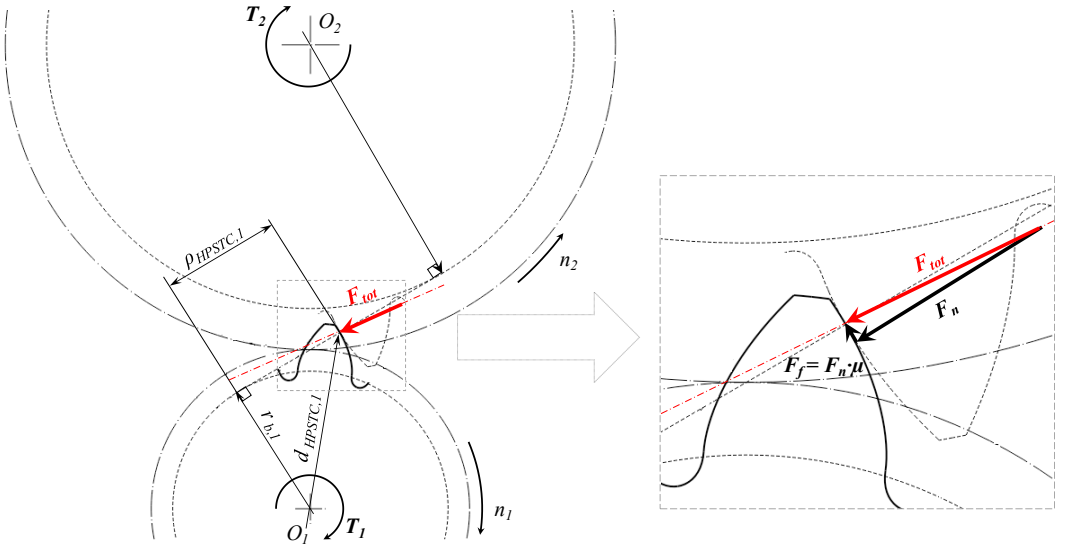

Figure 13. Forces acting at the HPSTC of a driver spur gear.

References

Baud, S., & Velex, P., 2002. Static and Dynamic Tooth Loading in Spur and Helical Geared Systems-Experiments and Model Validation. Journal of Mechanical Design, 124(2), 334.

Bower, A. F., 1988. Influence of crack face friction and trapped fluid on surface initiated rolling contact fatigue cracks. Journal of Tribology, 110(4), 704–711.

Handschuh, R. F., 1997. Recent advances in the analysis of spiral bevel gears. Cleveland, Ohio: TM-107391.

Hidaka, T., & Terauchi, Y. 1976. Dynamic Behavior of Planetary Gear : 1st Report Load Distribution in Planetary Gear. Bulletin of JSME, 19(132), 690–698.

Hotait, M. A., Kahraman, A., & Nishino, T., 2011. An Investigation of Root Stresses of Hypoid Gears with Misalignments. Journal of Mechanical Design, 133(7).

ISO 6336:2006 Calculation of load carrying capacity of spur and helical gears. 2006.

Johnson, K. L., 1987. *Contact Mechanics*. Cambridge University Press.

Krantz, T. L., 1992. Gear tooth stress measurements of two helicopter planetary stages. In "*Sixth International Power Transmission and Gearing Conference*". Phoenix, Arizona.

Ligata, H., Kahraman, A., & Singh, A., 2008. An Experimental Study of the Influence of Manufacturing Errors on the Planetary Gear Stresses and Planet Load Sharing. Journal of Mechanical Design, 130(4), 041701.

Oswald, F. B., 1987. Gear Tooth Stress Measurements on the UH-60A Helicopter Transmission. NASA Technical Paper, 2698, 17 p.

Pethick, J. A., 1967. *The construction and use of a test machine to measure dynamic loads on gear teeth.* Thesis (M.S. in Mechanical Engineering), United States Naval Academy.

Utagawa, M., & Harada, T., 1961. Dynamic Loads on Spur Gear Teeth at High Speed : Influence of the Pressure Angle Errors and Comparison between the Reduction Gears and the Speed-up Gears. Bulletin of JSME, 4(16), 706–713.

Yeh, B. H.-L., 1959. *Dynamic loads on spur gear teeth.* Thesis (M.S. in Applied Sciences),University of British Columbia.

Zhou, C., Hu, B., Chen, S., & Ma, L., 2016. Wireless measurement and dynamic contact analysis on the root stress of a light-load spur gear drive. Australian Journal of Mechanical Engineering, 1–9.